

Evaluation Strategies for Metal Artifact Reduction Approaches in CT: a Literature Survey

Mehrsima Abdoli^{1,*}

1. Department of Radiation Oncology, The Netherlands Cancer Institute, Amsterdam, The Netherlands.

Article info:

Received: February 03 2013

Accepted: February 28 2013

Keywords:

CT,
Metal Artifact Reduction,
Evaluation Metrics.

ABSTRACT

Metal-induced artifacts are known to degrade CT image quality and deteriorate the quantitative value of the images. Therefore, numerous metal artifact reduction techniques have been proposed and their performances have been evaluated using different qualitative or quantitative approaches. Various approaches and measures have been applied for the validation process visual assessment of the corrected images being one of the most commonly applied techniques. A high proportion of the presented techniques are not properly validated in the clinical environment, which hampers an unbiased comparison of the techniques and as such the clinical acceptability of the techniques remains questionable. Accurate quantitative evaluation of the processed images guarantees the reliability of the correction method. The main motivation of this work was to present the qualitative and quantitative validation approaches and metrics used in various metal artifact reduction studies in both phantom and clinical experiments. Considering the challenging task of validation of the clinical studies, where the gold standard is not present, having a proper knowledge about the potential solutions would assist the researchers to apply the right validation approaches.

1. Introduction

Computed tomography (CT) is one of the most widely used imaging modalities in the past decades in a wide range of medical applications. In radiation oncology CT images are conveniently used for treatment planning, patient positioning and dose calculations [1]. Beside its diagnostic values as a standalone imaging modality, its combination with positron emission tomography (PET) has improved the performance of this powerful functional imaging modality both qualitatively and quantitatively. CT-based attenuation correction of PET is the most clinically accepted attenuation correction technique which allows more accurate quantification of PET data [2, 3].

In spite of the substantial value of CT in various clinical applications, this image modality suffers from a number of known pitfalls and artifacts [4]. Metal-induced artifacts are one of the most common artifacts in CT images which are caused by metallic implants within the patients' body, such as cardiac defibrillators and pacemakers, dental fillings, hip and knee prostheses [5]. High atomic number of metallic objects severely attenuates the x-ray photons, which in turn generates gaps in the projection data. The appearance of streaking artifacts on reconstructed CT images is the obvious consequence of using such incomplete data for image reconstruction [6, 7].

The origin of metal streaking artifacts has been associated to several physical phenomena, such as noise,

** Corresponding Author:*

Mehrsima Abdoli, PhD

Department of Radiation Oncology, The Netherlands Cancer Institute, Amsterdam, The Netherlands.

Tel: +31 6 3989 9841

E-mail: mehrsima.abdoli@gmail.com

scatter, partial volume effect, object motion and beam hardening [8]. Since some or all of these phenomena are typically present when CT scans of objects with metallic compartments are made, the streaking artifacts are almost always generated on such CT scans. Generation of these bright and dark streaking artifacts deteriorate diagnostic qualitative and quantitative value of CT images. In radiotherapy, the presence of streaking artifacts obscures the anatomical structures, which precludes confident diagnosis of the disease and delineation of the organs for treatment planning. Moreover, the application of CT images including streaking artifacts in CT-based attenuation correction of PET data results in propagation of the artifacts into the corresponding PET images. Such artifacts might appear as over-estimated or under-estimated activity concentration regions which might lead to a false diagnosis of the disease. Therefore, the reduction of metallic artifacts has been a hot research topic in the past decade and several approaches, with various levels of success, have been proposed [9].

The proposed metal artifact reduction (MAR) approaches are generally categorized as implicit and explicit approaches. Most of the presented methods, however, lie in the explicit category, which involve various techniques for artifact reduction either in sinogram domain or image domain. A recent review on a broad range of MAR methods revealed that the sinogram-based methods tend to achieve more accurate processed images compared to image-based approaches [9]. Applying an interpolation-based algorithm combined with extra non-interpolation based corrections is reported as the most appropriate sinogram-based correction approach. However, accurate and precise validation of the techniques, particularly in the clinical setting where no ground truth is present, still remains a challenging task. In this paper, evaluation metrics and strategies used by the developers of the MAR techniques are presented and discussed.

2. Metal Artifact Reduction Evaluation Strategies

The performances of the various MAR approaches are assessed using a number of qualitative and quantitative methods and metrics. An accurate quantitative evaluation of the techniques in the clinical environment has always been a challenge due to the absence of the gold standard. Phantom studies are considered as an alternative and can offer reliable assessment, provided that the phantom design is realistic and analogous to the clinical situation. Table 1 summarizes all the validation techniques used in the literature and a detailed explanation is presented in the following subsections.

2.1. Phantom-Based Strategies

Phantom studies are the most common quantitative validation approach in the absence of gold standard. In case of MAR validation, since the actual Hounsfield unit of the patient body is not known, which makes quantitative analysis of the clinical data impractical, making CT images of phantoms can serve as an alternative. Physical or simulated phantoms have been widely used for MAR evaluation [10-17]. The phantoms used in different studies range from a simple simulated jaw phantom [13] to more complex phantoms, such as anthropomorphic phantom [18]. It is evident that the phantoms designed more analogous to the real clinical data result in a more precise and reliable validation. However, the evaluation metrics and measures used to quantify the analysis also play an important role in the validation process. Although in some few studies the phantom experiments are assessed only visually [18-22], which is most probably sufficient for the specific purpose of the presented works, the application of proper assessment metrics has undoubtedly an added value in the course of validation. Wherever a visual qualitative assessment is applied, the preservation of the fine structures surrounding the metallic object and the extent of the artifact reduction in that area is noticed.

A simple and common approach in phantom-based evaluation of MAR approaches is the comparison of mean and standard deviation (SD) of the intensities within specified regions of interest (ROIs) [10, 17, 23-25]. Comparing the SD of regions provides information about the discrepancy between CT numbers of similar regions before and after correction. In such cases, the finest practice is to define several ROIs in regions corresponding to different tissues and to report the differences both in artifactual and artifact-free areas. Plotting the line profiles passing through different regions of the phantom images before and after correction as well as the artifact-free image can serve as a visual assistance to perceive the HU differences [14, 26-28]. The line profile of the original phantom image without inserting metallic objects is expected to have a relatively uniform intensity distribution and the deviations of the artifactual and corrected profiles from this line profile represents the bias. Figure 1 represents the CT images of a cylindrical polyethylene phantom with 16 inserts which simulate different tissues in human body. The artifact-free image (top left) is taken while no metallic object was inserted into the phantom and this image serves as the gold standard. Top middle presents the CT image with the metallic inserts, and the top right shows the corresponding metal artifact corrected image. Line profiles from the same

regions of the three images are plotted in figure 1 and the fluctuations due to the streaking artifacts before and after correction (blue and red lines, respectively) can be compared to the ground truth (green line). A statistical analysis, such as 2-tailed paired t-test, might also be applied to emphasize the statistical significance of the intensity variation before and after correction [29, 30].

The pixel histograms plotted for different tissue components of the phantom is another approach which can

contribute in both visual and quantitative analysis of the changes in the pixel intensities of the images before and after correction and compare those to the ground truth [10, 31].

Mean relative error (MRE), mean squared error (MSE) and root mean square error (RMS) are three prevalent metrics to evaluate the difference between the two measures and have been extensively used for MAR validation [13, 16, 31-35]. They are generally defined as follows:

Table 1. Summary of the validation techniques used in the literature for evaluation of MAR approaches

Phantom-based strategies	Qualitative	<ul style="list-style-type: none"> Preservation of the fine structures Extent of the artifact reduction Smoothness and continuity of the sinogram or its isophotes
	Qualitative	<ul style="list-style-type: none"> General Applications <ul style="list-style-type: none"> Plots <ul style="list-style-type: none"> Line profiles passing through different regions Pixel histograms for different tissue components Measures of errors <ul style="list-style-type: none"> Mean relative error Mean squared error Root mean square error Mean percent absolute error Other <ul style="list-style-type: none"> Mean and standard deviation within selected ROIs Mean I divergence Signal-to-background ratio Contrast-to-noise-ratio Specific Applications <ul style="list-style-type: none"> CTAC of PET <ul style="list-style-type: none"> Comparison of activity concentration Target-to-background ratio Radiotherapy Treatment Planning <ul style="list-style-type: none"> Percentage error in dose calculations
Strategies based on clinical data	Qualitative	<ul style="list-style-type: none"> General Applications <ul style="list-style-type: none"> Borders of the organs surrounding the metallic objects Edge preserving of the metallic objects and the surrounding organs Overall diagnostic value of the images Specific Applications <ul style="list-style-type: none"> CTAC of PET <ul style="list-style-type: none"> Comparison of CT-based attenuation corrected PET with the one which is not corrected for attenuation Comparison of the CT-based attenuation corrected PET with the one attenuation corrected using the conventional transmission scan Radiotherapy Treatment Planning <ul style="list-style-type: none"> Comparison of the isodose distribution before and after correction
	Quantitative	<ul style="list-style-type: none"> General Applications <ul style="list-style-type: none"> Assumed/simulated gold standards <ul style="list-style-type: none"> Manual segmentation of a test set Simulation of streaking artifacts on artifact-free real clinical datasets Use of adjacent slice with no artifact as the ground truth Regression without truth Metrics based on presence of the ground truth <ul style="list-style-type: none"> Normalized total variation error Normalized root mean square difference Mean absolute deviation Other <ul style="list-style-type: none"> Image qualities scored by two radiologists Image entropy Subtraction of the images Comparing the performance of proposed technique with the already existing ones Specific Applications <ul style="list-style-type: none"> Radiotherapy Treatment Planning <ul style="list-style-type: none"> Percentage error in dose calculation between the original and corrected CT

$$\% MRE = \frac{I^{measured} - I^{true}}{I^{true}} \times 100 \quad (1)$$

$$RMS = \sqrt{\frac{\sum_{i=1}^N (I^{measured}(i) - I^{true}(i))^2}{N}} \quad (3)$$

$$MSE = \frac{1}{N} \sum_{i=1}^N (I^{measured}(i) - I^{true}(i))^2 \quad (2)$$

where I^{true} is the ground truth image, $I^{measured}$ is the image which is compared to the ground truth (i.e. the artifactual or corrected image), i indexes the individual pixels and N denotes the total number of pixels within the ROIs.

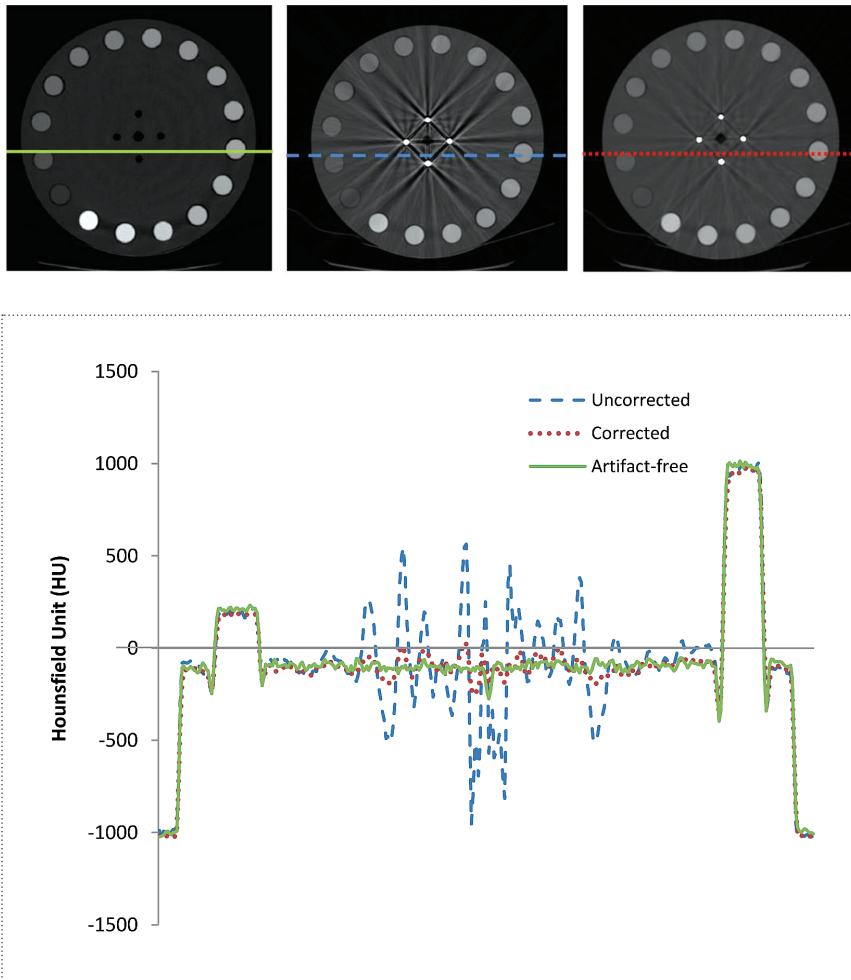


Figure 1. Validation of MAR using line profiles. The CT images from left to right illustrate the artifact-free (i.e. without metal inserts), uncorrected image (with metal inserts) and the corrected image. The corresponding line profile of each image is plotted for comparison.

Other quantitative measures of difference used in the literature include mean percent absolute error (MPAE) and mean I divergence (Mean I-div) [34], which are defined as:

$$MPAE = \frac{1}{N} \sum_{i=1}^N \left| \frac{I^{measured}(i)}{I^{true}(i)} - 1 \right| \quad (4)$$

$$Mean I - div = \frac{1}{N} \sum_{i=1}^N \left(I^{true}(i) \cdot \ln \left[\frac{I^{true}(i)}{I^{measured}(i)} - I^{true}(i) + I^{measured}(i) \right] \right) \quad (5)$$

where the latter quantifies the discrepancy between the two measures.

Measurement of signal-to-background ratio (SNR) and contrast-to-noise-ratio (CNR) of the corrected image and comparing to that of the ground truth might also provide extra information about the performance of the MAR algorithm [36, 37]. Ideally, after applying a MAR algorithm, one would expect to achieve the same SNR and CNR of the gold standard, and such comparison of the two measures might be worthwhile.

The assessment strategy might also be pursued in the sinogram domain. Visual assessment of the smoothness and continuity of the sinogram or its isophotes before and after correction has been used in the literature as an alternative assessment scheme [32, 38-40].

In some studies, where the proposed MAR is meant for a specific practice, the evaluation procedure is adapted to the planned goal. In CT-based attenuation correction of PET data, for instance, the validation can be performed on the PET images. When a phantom study has been carried out, the actual activity concentration in the phantom is known, and as such the performance of

the algorithm can be accurately assessed [12, 32, 41]. Target-to-background ratio (TBR) can also be used as a quantitative measure in such cases [15]. Moreover, when the MAR algorithm is meant to improve the radiotherapy treatment planning and dose calculations, the percentage error in dose calculations is considered as a valid evaluation metric [11].

2.2. Strategies Based on the Clinical Data

Although phantom studies are appreciated and must be considered as an essential step for MAR validation, in order to have the proposed technique clinically acceptable, it has to be validated using the clinical datasets to see how the method performs in real life. The adversity associated with the clinical studies is the lack of the ground truth. It is known that the dark and bright streaking artifacts should disappear after correction, but whether the correct Hounsfield unit is assigned to the human tissue after correction, is not known. As explained earlier, for many clinical applications of CT images, it is important to achieve valid CT numbers after correction and as such, quantitative assessment of the clinical datasets is essential. However, due to the absence of the ground truth, a high proportion of

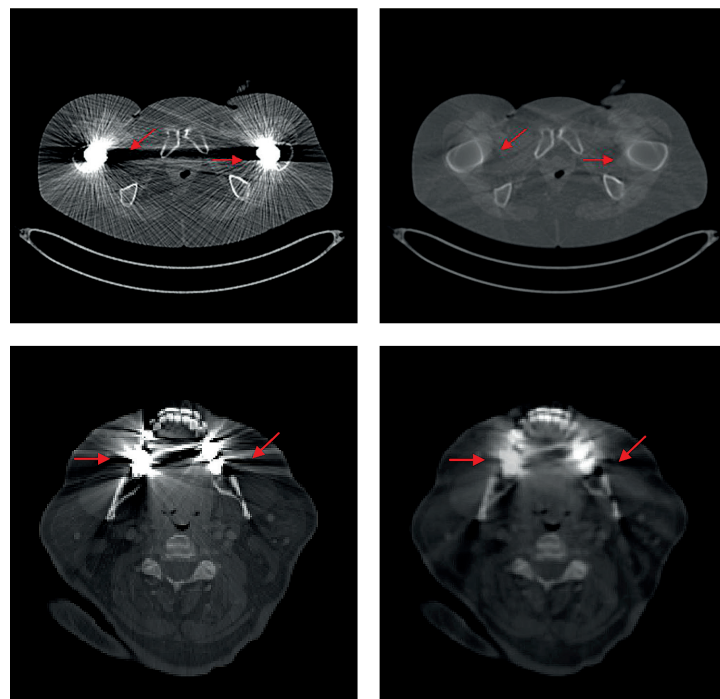


Figure 2. Two sample clinical CT images of patients with hip prosthesis (top) and dental filling (bottom) before (left) and after (right) metal artifact reduction. The red arrows are pointing at the borders of the organs surrounding the metal implant.

the presented works are evaluated only qualitatively [10, 14, 15, 17, 23, 26, 27, 31, 42-45]. For the qualitative assessment, a high attention is paid to the borders of the organs surrounding the metallic objects, to the edge preserving of the metallic objects and the surrounding organs, and the overall diagnostic value of the images after correction. Figure 2 illustrates a sample clinical CT image before and after metal artifact reduction. The red arrows are pointing at some organ borders which are obscured by the artifacts before correction, while on the other hand are obviously observable after correction.

There have been a number of studies in which the authors attempted to find a strategy for quantitative assessment of the clinical data, even though the gold standard is not known. Mahnken et al. got the image qualities scored by two radiologists and analyzed the results using a repeated measure ANOVA statistical analysis [29]. A similar approach was applied by Mersbach et al., where the axial, coronal and sagittal views of the CT scans were evaluated by two blinded and independent observers [46]. The evaluation was conducted based on the overall image quality, with a specific attention to the quality of pelvic organs and assessment of pelvic abnormalities. Moreover, CT attenuation and image noise were measured before and after correction. The results were statistically analyzed using the Friedman test, Wilcoxon signed-rank test and Levene test.

Another analytical approach is the manual segmentation of a test set by the experts, which can serve as the ground truth [47]. The test set is, then, processed by the proposed MAR approach and the resulting images are compared to the ground truth using the Jaccard and Dice index.

Image entropy is another quantitative measure used for evaluation of MAR methods [48]. Image entropy is calculated as follows:

$$h = \sum_{g \in G} q_g \log(q_g) \quad (6)$$

where q_g is the portion of image pixels with intensity of g . The entropy of the image is a measure for intensity variations and when applied to the processed images, it measures the additional variation induced by streaking artifacts. Whenever the variations are caused by the regular variability of the intensities of the anatomical structures, the entropy is maximized. Therefore, this measure can also be used to optimize the performance of the MAR techniques by incorporating an algorithm parameter into the entropy formulation and maximizing it.

Another interesting approach to validate the MAR technique in the clinical setting is to use an artifact-free clinical dataset and simulate realistic streaking artifacts on the images. In this way the ground truth is available for an accurate quantitative validation. This method has been proposed by Mehranian et al [49-51]. The validation metric used in their study is the normalized total variation error (%TV) which is an indicator of the amount of artifacts in the reconstructed images:

$$\%TV = 100 \times \left(\frac{\|\nabla(I^{simulated} - I^{true})\|_1}{\|\nabla I^{true}\|_1} \right) \quad (7)$$

where $I^{simulated}$ is the image with the simulated artifact and I^{true} is the ground truth. Normalized root mean square difference (NRMSD) and mean absolute deviation (MAD) between the corrected image ($I^{corrected}$) and the ground truth are the other two metrics used in the studies with simulated artifacts on the clinical data:

$$\%NRMSD = 100 \times \sqrt{\frac{\sum_{i \in ROI} (I_i^{corrected} - I_i^{true})^2}{\sum_{i \in ROI} (I_i^{true})^2}} \quad (8)$$

$$MAD = \frac{1}{N} \sum_{i \in ROI} |I_i^{corrected} - I_i^{true}| \quad (9)$$

where MAD is reported in HU.

A less quantitative comparison approach is the subtraction of the images before and after correction and tracking the considerable differences on the organs of interest [52]. This method might be applied more quantitatively if an adjacent slice with no artifact (or negligible amount of artifact) can be found in the database which consists of similar anatomical structures to that of the artifactual slice. In such case, the artifact-free slice can be considered as the ground truth. The visual assessment of the subtraction of the artifact-free slice and the corrected image is the validation technique of choice in a study conducted by Dong et al. [53].

In case of CT-based attenuation of PET data, the PET image which is attenuation corrected by the artifact reduced CT can be compared to the one which is not corrected for attenuation [54]. However, this comparison

cannot be analyzed quantitatively due to the fact that the quantification of the PET data without attenuation correction is known to be very inaccurate. Comparison of the CT-based attenuation corrected PET with the one attenuation corrected using the conventional transmission scan is another way of validation for this application of CT in nuclear medicine [12].

A clinical approach for validation of the MAR performance when CT is being used for radiotherapy treatment planning is the comparison of the isodose distribution before and after correction. This approach has been applied in a study by Xu et al. [28]. Percentage error in dose calculation between the original and corrected CT is another measure in this specific application [11].

Hoppin et al. proposed a validation technique in the absence of gold standard, which is known as regression without truth (RWT) [55]. The technique is meant to compare the performance of two modalities with the presumed gold standard and to show which modality performs more similar to the ground truth. It calculated a figure of merit (FOM) for each modality based on the parameters of a linear relationship between the true value of the parameter which we are interested in, and its estimated value. The two FOMs are, then, compared and the modality with smaller FOM is concluded to perform more similar to the ground truth. This method can be conveniently used for validation of MAR in the clinical environment, without being concerned about the absence of gold standard [39, 56].

Alongside all the validation approaches, comparing the performance of any proposed technique with the already existing ones is a common method to prove the added value of the novel techniques [22, 43, 44, 57]. The comparison per se is not considered as a validation tool, and is rather used as a complementary process.

3. Discussion and Conclusion

The necessity of metal artifact reduction on CT images has been shown in many studies [9]. However, a high fraction of all proposed MAR methods are poorly validated in the clinical setting. This article attempts to provide the community with all the quantitative approaches used for the validation of the proposed MAR techniques, using both phantom and clinical studies. The choice of quantitative metric for validation purposes, however, is not a trivial question to answer, which is the case in all research areas. In order to achieve the clinical acceptance, the application of various quantitative validation metrics is commendable.

The methods which assist better visualization of the differences before and after correction, such as line profiles and histograms, are proper tools for primary analysis of the data. These methods, however, must be followed by more in-depth quantitative analysis. The measures of error and differences can be conveniently used in phantom studies. For the clinical studies, due to the lack of the ground truth, these measures cannot be directly applied. As shown in section II, in spite of lack of gold standard in the clinical environment, there has been a number of quantitative validation approaches used to validate the MAR techniques in the clinical setting. The proposed techniques, which provide a substitution for the gold standard, might become beneficial in such cases. Using the adjacent artifact-free slice, simulation of the artifacts on real artifact-free clinical images, and application of RWT method have been used to tackle the no-gold-standard issue. Several other validation metrics are also proposed which might help to improve the accuracy and precision of the validation procedure.

Although some MAR methods are designed for specific purposes in which qualitative validation of the performance of MAR method would be sufficient, a successful MAR, which can be accepted and implemented in the clinic, is the one which is qualitatively and quantitatively valid. This highlights the need for a more accurate quantitative evaluation of the proposed approaches. The visual assessment of the processed images by experts, however, would definitely improve the validation as a complementary process.

Considering all the available validation tools, a fairly designed validation process must consist of accurate quantitative evaluation of one or more phantom studies as well as qualitative and quantitative assessment of a number of clinical studies, using various validation metrics. The application of the same framework in all research groups would be beneficial for an unbiased comparison of the MAR performances, which would make the clinical applicability of the techniques with superior performance feasible.

References

- [1] J. J. Battista, et al., "Computed tomography for radiotherapy planning," *International journal of radiation oncology, biology, physics*, vol. 6, pp. 99-107, 1980.
- [2] B. H. Hasegawa and H. Zaidi, "Dual-Modality Imaging: More Than the Sum of its Components," in *Quantitative Analysis in Nuclear Medicine Imaging*, H. Zaidi, Ed., ed: Springer, 2006, pp. 53-54.
- [3] P. E. Kinahan, et al., "Attenuation correction for a combined 3D PET/CT scanner," *Med Phys*, vol. 25, pp. 2046-53, Oct 1998.
- [4] J. F. Barrett and N. Keat, "Artifacts in CT: recognition and avoidance," *Radiographics*, vol. 24, pp. 1679-91, Nov-Dec 2004.
- [5] E. Klotz, et al., "Algorithms for the reduction of CT artifacts caused by metallic implants," *Proc. SPIE*, vol. 1234, pp. 642-650, 1990.
- [6] D. D. Robertson, et al., "Total Hip Prosthesis Metal-Artifact Suppression Using Iterative Deblurring Reconstruction," *Journal of Computer Assisted Tomography*, vol. 21, pp. 293-298, 1997.
- [7] W. A. Kalender, et al., "Reduction of CT Artifacts Caused by Metallic Implants," *Radiology*, vol. 164, pp. 576-577, 1987.
- [8] B. de Man, et al., "Metal streak artifacts in X-ray computed tomography: a simulation study," *IEEE Trans Nucl Sci*, vol. 46, pp. 691-696, 1999.
- [9] M. Abdoli, et al., "Metal artifact reduction strategies for improved attenuation correction in hybrid PET/CT imaging," *Med Phys*, vol. 39, pp. 3343-60, Jun 2012.
- [10] M. Bal and L. Spies, "Metal artifact reduction in CT using tissue-class modeling and adaptive prefiltering," *Med Phys*, vol. 33, pp. 2852-9, Aug 2006.
- [11] M. Bazalova, et al., "Correction of CT artifacts and its influence on Monte Carlo dose calculations," *Med Phys*, vol. 34, pp. 2119-32, Jun 2007.
- [12] J. J. Hamill, et al., "A knowledge-based method for reducing attenuation artefacts caused by cardiac appliances in myocardial PET/CT," *Phys Med Biol*, vol. 51, pp. 2901-18, Jun 7 2006.
- [13] S. Aootaphao, et al., "Penalized-likelihood reconstruction for metal artifact reduction in cone-beam CT," presented at the *Engineering in Medicine and Biology Society*, 2008, Vancouver, British Columbia, Canada, 2008.
- [14] J. Hsieh, et al., "An iterative approach to the beam hardening correction in cone beam CT," *Med Phys*, vol. 27, pp. 23-9, Jan 2000.
- [15] J. A. Kennedy, et al., "The reduction of artifacts due to metal hip implants in CT-attenuation corrected PET images from hybrid PET/CT scanners," *Med Biol Eng Comput*, vol. 45, pp. 553-62, Jun 2007.
- [16] B. Kratz and T. M. Buzug, "Metal artifact reduction in computed tomography using nonequispaced fourier transform," presented at the *Nuclear Science Symposium Conference Record (NSS/MIC)*, 2009 IEEE, Orlando, Florida, 2009.
- [17] C. Lemmens, et al., "Suppression of metal artifacts in CT using a reconstruction procedure that combines MAP and projection completion," *IEEE Trans Med Imaging*, vol. 28, pp. 250-260, 2009.
- [18] J. Wei, et al., "X-ray CT high-density artefact suppression in the presence of bones," *Phys Med Biol*, vol. 49, pp. 5407-18, Dec 21 2004.
- [19] B. De Man, et al., "Reduction of metal streak artifacts in X-ray computed tomography using a transmission maximum a posteriori algorithm," *IEEE Transactions on Nuclear Science*, vol. 47, pp. 977-981, 2000.
- [20] X. Duan, et al., "Metal artifact reduction in CT images by sinogram TV inpainting," presented at the *Nuclear Science Symposium Conference Record*, 2008. NSS '08. IEEE, Dresden, Germany, 2008.
- [21] Y. Li, et al., "Metal artifact reduction in CT based on adaptive steering filter and nonlocal sinogram inpainting," in *Biomedical Engineering and Informatics (BMEI)*, 2010 3rd International Conference on, 2010, pp. 380-383.
- [22] E. Meyer, et al., "Normalized metal artifact reduction (NMAR) in computed tomography," *Med Phys*, vol. 37, pp. 5482-93, Oct 2010.
- [23] W. J. Veldkamp, et al., "Development and validation of segmentation and interpolation techniques in sinograms for metal artifact suppression in CT," *Med Phys*, vol. 37, pp. 620-8, Feb 2010.
- [24] J. Wu, et al., "Metal artifact reduction algorithm based on model images and spatial information," *Nuclear Instruments and Methods in Physics Research Section A: Accelerators, Spectrometers, Detectors and Associated Equipment*, vol. 652, pp. 602-605, 2011.
- [25] H. Yu, et al., "A segmentation-based method for metal artifact reduction," *Acad Radiol*, vol. 14, pp. 495-504, Apr 2007.
- [26] D. Prell, et al., "A novel forward projection-based metal artifact reduction method for flat-detector computed tomography," *Phys Med Biol*, vol. 54, pp. 6575-91, Nov 7 2009.
- [27] J. C. Roeske, et al., "Reduction of computed tomography metal artifacts due to the Fletcher-Suit applicator in gynecology patients receiving intracavitary brachytherapy," *Brachytherapy*, vol. 2, pp. 207-14, 2003.
- [28] C. Xu, et al., "An algorithm for efficient metal artifact reductions in permanent seed," *Med Phys*, vol. 38, pp. 47-56, Jan 2011.
- [29] A. H. Mahnken, et al., "A new algorithm for metal artifact reduction in computed tomography: in vitro and in vivo evaluation after total hip replacement," *Invest Radiol*, vol. 38, pp. 769-75, Dec 2003.
- [30] M. Abdoli, et al., "A virtual sinogram method to reduce dental metallic implant artefacts in computed tomography-based attenuation correction for PET," *Nucl Med Commun*, vol. 31, pp. 22-31, Jan 2010.
- [31] Y. Zhang, et al., "Reducing metal artifacts in cone-beam CT images by preprocessing projection data," *Int J Radiat Oncol Biol Phys*, vol. 67, pp. 924-32, Mar 1 2007.

- [32] M. Abdoli, et al., "Reduction of artefacts caused by hip implants in CT-based attenuation corrected PET images using 2D interpolation of a virtual sinogram on an irregular grid," *Eur J Nucl Med Mol Imaging*, vol. 38, pp. 2257-68, 2011.
- [33] M. Abdoli, et al., "Comparative assessment of image- and virtual sinogram-based metal artefact reduction techniques for CT-based attenuation correction in PET," *Eur J Nucl Med Mol Imaging*, vol. 36, p. S194, 2009.
- [34] J. F. Williamson, et al., "Prospects for quantitative computed tomography imaging in the presence of foreign metal bodies using statistical image reconstruction," *Med Phys*, vol. 29, pp. 2404-18, Oct 2002.
- [35] G. Delso, et al., "MR-driven metal artifact reduction in PET/CT," *Phys Med Biol*, vol. 58, pp. 2267-80, Apr 7 2013.
- [36] J. Rinkel, et al., "Computed tomographic metal artifact reduction for the detection and quantitation of small features near large metallic implants: a comparison of published methods," *J Comput Assist Tomogr*, vol. 32, pp. 621-9, Jul-Aug 2008.
- [37] X. Zhang, et al., "Metal artifact reduction in x-ray computed tomography (CT) by constrained optimization," *Med Phys*, vol. 38, pp. 701-11, Feb 2011.
- [38] M. Abdoli, et al., "Reduction of Dental Filling Metallic Artifacts in CT-Based Attenuation Correction of PET Data Using Weighted Virtual Sinograms," in *IEEE Nucl Sci Symp Conf Rec*, 2009, pp. 2752-2755.
- [39] M. Abdoli, et al., "Reduction of dental filling metallic artifacts in CT-based attenuation correction of PET data using weighted virtual sinograms optimized by a genetic algorithm," *Med Phys*, vol. 37, pp. 6166-6177, 2010.
- [40] J. Gu, et al., "X-ray CT metal artifacts reduction through curvature based sinogram inpainting," *Journal of X-Ray Science and Technology*, vol. 14, pp. 73-82, 2006.
- [41] M. Abdoli, et al., "Clough-Tocher interpolation of virtual sinogram in a Delaunay triangulated grid for metal artifact reduction of PET/CT images," in *Nuclear Science Symposium and Medical Imaging Conference (NSS/MIC)*, 2011 IEEE, 2011, pp. 3197-3201.
- [42] L. Cheng and J. Liu, "Metal Artifacts Reduction in Computed Tomography: A Bilateral Reprojection Approach," presented at the *Bioinformatics and Biomedical Engineering (iCBBE)*, 2010 4th International Conference on, Chengdu, 2010.
- [43] K. Y. Jeong and J. B. Ra, "Metal Artifact Reduction Based on Sinogram Correction in CT," presented at the *IEEE Nuclear Science Symposium Conference Record (NSS/MIC)*, Orlando, FL 2009.
- [44] H. Li, et al., "Metal artifact suppression from reformatted projections in multislice helical CT using dual-front active contours," *Med Phys*, vol. 37, pp. 5155-64, Oct 2010.
- [45] A. Kondo, et al., "Iterative correction applied to streak artifact reduction in an X-ray computed tomography image of the dento-alveolar region," *Oral Radiology*, vol. 26, pp. 61-65, 2010.
- [46] F. Morsbach, et al., "Reduction of metal artifacts from hip prostheses on CT images of the pelvis: value of iterative reconstructions," *Radiology*, vol. 268, pp. 237-44, Jul 2013.
- [47] V. Naranjo, et al., "Metal artifact reduction in dental CT images using polar mathematical morphology," *Comput Methods Programs Biomed*, vol. 102, pp. 64-74, Apr 2011.
- [48] M. Oehler and T. M. Buzug, "The λ -MLEM Algorithm: An Iterative Reconstruction Technique for Metal Artifact Reduction in CT Images," in *Advances in Medical Engineering*, vol. 114, ed: Springer Berlin Heidelberg, 2007, pp. 42-47.
- [49] A. Mehranian, et al., "Metal artifact reduction in CT-based attenuation correction of PET using sobolev sinogram restoration," presented at the *Nuclear Science Symposium and Medical Imaging Conference (NSS/MIC)*, 2011 IEEE, Valencia, Spain, 2011.
- [50] A. Mehranian, et al., "Sparsity constrained sinogram inpainting for metal artifact reduction in x-ray computed tomography," in *Nuclear Science Symposium and Medical Imaging Conference (NSS/MIC)*, 2011 IEEE, 2011, pp. 3694-3699.
- [51] A. Mehranian, et al., "3D Prior Image Constrained Projection Completion for X-ray CT Metal Artifact Reduction," *Nuclear Science, IEEE Transactions on*, vol. 60, pp. 3318-3332, 2013.
- [52] G. H. Glover and N. J. Pelc, "An algorithm for the reduction of metal clip artifacts in CT reconstructions," *Med Phys*, vol. 8, pp. 799-807, Nov-Dec 1981.
- [53] J. Dong, et al., "Successive iterative restoration applied to streak artifact reduction in X-ray CT image of dento-alveolar region," *Int J Comput Assist Radiol Surg*, Jan 5 2011.
- [54] J. Nuyts and S. Stroobants, "Reduction of attenuation correction artifacts in PET-CT," *IEEE Nuclear Science Symposium Conference Record*, vol. 4, pp. 1895-1899, 23-29 Oct. 2005 2005.
- [55] J. W. Hoppin, et al., "Objective Comparison of Quantitative Imaging Modalities Without the Use of a Gold Standard," in *IEEE Trans Med Imag*, 2002, pp. 441-449.
- [56] M. Abdoli, et al., "Optimization of weighted virtual sinogram-based metal artifact reduction in CT-based attenuation correction of PET data using a genetic algorithm," *Eur J Nucl Med Mol Imaging*, vol. 37, p. S285, 2010.
- [57] Y. Kim, et al., "Effective sinogram-inpainting for metal artifacts reduction in X-ray CT images," presented at the *Image Processing (ICIP)*, 17th IEEE International Conference on, Hong Kong, 2010.